Red fox genome assembly identifies genomic regions associated with tame and aggressive behaviors

Anna V. Kukekova[1*], Jennifer L. Johnson[1], Xueyan Xiang[2], Shaohong Feng[2], Shiping Liu[2], Halie M. Rando[1], Anastasiya V. Kharlamova[3], Yury Herbeck[3], Natalya A. Serdyukova[4], Zijun Xiong[2,5], Violetta Beklemischeva[4], Klaus-Peter Koepfli[6,7], Rimma G. Gulevich[3], Anastasiya V. Vladimirova[3], Jessica P. Hekman[1], Polina L. Perelman[4,8], Aleksander S. Graphodatsky[4,8], Stephen J. O'Brien[8,9], Xu Wang[10#], Andrew G. Clark[10], Gregory M. Acland[11], Lyudmila N. Trut[3], Guojie Zhang[2,5,12*]

Contents

Supplementary Table 9. PANTHER overrepresentation statistics.

Supplementary Table 10. Identification of brain expressed genes both from significant windows and a complete list of annotated genes in 9,151 windows.

Supplementary Table 11. Genes from significant windows identified in KEGG database for glutamatergic, serotonergic, dopaminergic, GABAergic, and cholinergic synapses.

Supplementary Table 12. Genomic regions identified in the analysis of pooled heterozygosity (*Hp*) and fixation index (F_{ST}).

Supplementary Table 13. Comparison of 103 regions of interest identified in the fox with regions under selection in dogs.

Supplementary Table 14. Fox QTL that overlap with 103 genomic regions from Supplementary Table 7.

Supplementary Table 15. Fox orthologs of genes associated with autism spectrum disorders and bipolar disorder in humans and/or found to affect aggression in mouse models that were identified in significant *Hp* and F_{ST} windows.

Supplementary Table 16. Pooled heterozygosity analysis in the region partly syntenic to the Williams-Beuren syndrome region in humans.

Supplementary Table 17. Missense mutations identified in *CACNA1C, ATP10A, MYO9B, IQGAP2,* and *PTPRO* genes.

Supplementary Table 18. The genes associated with human behavioral disorders that were highlighted in this study.

Supplementary Table 19. Primer pairs and multiplexes used for genotyping the 5-Mb region on VVU15.

Supplementary Table 20. Haplotypes identified in the 5-Mb interval on VVU15.

Supplementary Table 21. Statistics of the STRUCTURE analysis.

Supplementary Table 22. Fox SNPs identified using the dog genome as a reference.

Supplementary Note 1. Simulation of allelic fixation.

Simulations were performed to estimate the rate of allelic fixation expected in a population demographically similar to the tame population but bred with no influence of selection. The results of the simulation study were also used to estimate an appropriate window size for the selective sweep scan and to validate the cut-off for the pooled heterozygosity (*Hp*) analysis of the fox populations. The simulations were run for a variety of scenarios under realistic recombination rates using the program forqs (Kessner and Novembre, 2014). Forqs generates haplotypes in the founding generation and then follows them through each generation of the simulation, allowing them to recombine according to the parameters specified. The data generated for the final generation indicate which haplotypes are identical-by-descent with founder haplotypes at each position along the chromosome. This approach allowed us to look at both the frequencies of the founding haplotypes in the final generation and the lengths of the haplotypes after multiple generations of recombination.

Simulation scenarios

Population parameters were selected for the simulation based on pedigree information and breeding records from 1959 (when the population was founded) through 2010, as the DNA samples used in the current study were collected no later than 2010. Foxes reproduce once per year, but the majority of breeding animals are bred for several years, leading to overlapping generations. We simulated 50 generations of breeding, although the overall number of generations in the experimental population was expected to be lower. The tame population originated from 198 founders and included approximately 200 breeding animals in each generation. Because the simulations model an equal chance of breeding among all animals, we had to use a population size larger than 200 in order to simulate 200 breeders. If every animal has an equal chance of mating in a given generation, some animals will mate more than once and some will not get a chance to mate, so in order to reflect the known average number of animals that mated in each generation in the population being simulated, we calculated that a population size of 240 would yield about 200 animals breeding in each generation.

To approximate the tame population, a base model was simulated using 240 unrelated individuals (480 haplotypes) that were bred for 50 generations without selection. The assumptions made about the fox population in the model were then evaluated by modifying

each of three parameters: (1) population size, (2) level of relatedness among the breeding animals, and (3) the number of generations. Each simulation scenario (9 scenarios, total) was replicated 100 times. Each of the parameters was evaluated as follows:

1. To evaluate the effect of population size, three population sizes of 120, 480, and 960 individuals were modeled. Each of these scenarios assumed that every founder had two unique haplotypes and that the population was bred for 50 generations.

2. To evaluate the effect of the relatedness of the founding animals, two alternate levels of relatedness were simulated. The populations were set to have either 50 or 100 founding haplotypes distributed evenly in the first generation, in contrast to the 480 in the base simulation. In these scenarios, populations of 240 individuals were bred for 50 generations.

3. To evaluate the effect of the number of generations, breeding of the base population (240 unrelated individuals) was simulated over 100, 250, and 500 generations.

The simulations were run using fox chromosome 1 (VVU1) as a proxy for the fox genome. The chromosomal length (220 Mb) and recombination map (120 cM) were approximated using a meiotic linkage map of VVU1 aligned against the dog genome (Kukekova et al., 2012). Fox autosomes are metacentric, and the recombination rate varies significantly along the chromosomes (Kukekova et al., 2007, 2012). The centimorgan (cM) to megabase (Mb) ratios along VVU1 varied from 4 and 5 cM per Mb on the chromosome ends to 0.07 cM per Mb in the pericentromeric region (Supplementary Figure 3). The recombination pattern has been slightly adjusted to smooth the recombination frequency curve and to extrapolate the cM to Mb ratios for the very ends of the chromosome as required by forqs.

Estimation of haplotype frequencies in simulated populations.

Haplotype frequencies were calculated at 100,000-bp intervals in each simulation scenario. The distribution of the haplotype frequencies (Supplementary Figure 4) included all non-zero haplotype frequencies across all 100 replications of each scenario. The plots and graphs show the distribution of the haplotype frequencies under each simulation scenario. The maximum haplotype frequencies and, when applicable, the proportion of the genome that reached fixation in the final generation are summarized for each simulation scenario in Note Table 1.

Note Table 1. The results of the simulation for the base case and when population size, starting number of haplotypes, or the number of generations were modified. Each row represents a simulation scenario. Each simulation scenario differs from the base model by one parameter, which is highlighted.

Parameter tested	Simulation scenario	Population size	Number of starting haplotypes	Number of generations	Maximum haplotype frequency	Proportion of genome fixed
Base Model	**1**	**240**	**480**	**50**	**0.521**	**N/A**
Population size	2	120	240	50	0.846	N/A
	3	480	960	50	0.314	N/A
	4	960	1,920	50	0.186	N/A
Number of starting haplotypes	5	240	50	50	0.600	N/A
	6	240	100	50	0.644	N/A
Number of generations	7	240	480	100	0.844	N/A
	8	240	480	250	1.000	0.0042*
	9	240	480	500	1.000	0.1393*

** The proportion of the genome that was fixed was calculated separately for each scenario by summing the total lengths of all fixed haplotypes in all individuals in 100 replications and dividing by the total length of all chromosomes investigated (the chromosome length (220 Mb) analyzed in 100 replicates for all individuals).*

In the base model (240 unrelated individuals bred for 50 generations without selection), the maximum haplotype frequency observed was 0.521 (Note Table 1; simulation scenario 1). When a smaller population size or a smaller number of founding haplotypes were simulated the maximum haplotype frequencies in the final generation increased but did not reach fixation in either scenario (Note Table 1; simulation scenarios 2-6). The only parameter that caused any haplotypes to reach fixation was the number of generations when it was set to 250 and 500 (Note Table 1; simulation scenarios 8 and 9). These results indicate that even under most conservative assumptions (simulation scenarios 2 and 5), it is unlikely for haplotype fixation to occur by chance after 50 generations of breeding.

Estimation of an appropriate cut-off for pooled heterozygosity (Hp) analysis

In order to evaluate the pooled heterozygosity (*Hp*) cut-off used for a selective sweep scan in the fox populations, we computed the theoretical *Hp* for the haplotype frequencies obtained in simulation scenarios with 50 generations of breeding (Note Table 1; simulation scenarios 1-6).

In the pooled heteroygosity analysis, *Hp* was computed according Rubin et al., 2010 (formula 1) by examining all SNPs in a specified genomic window using the pooled sequencing of the individuals from each population and summing the number of sequencing reads from major and minor alleles represented in the window. The pooled approach minimizes the effects of sequencing errors and random sequencing on any given SNP and provides an estimate of the level of heterozygosity found in that region of the genome. Because the simulations returned data as haplotype frequencies, not individual SNP genotypes, we modified the formula to estimate the highest theoretical *Hp* value that would be expected based on the haplotype frequencies observed in the neutral simulations.

To simplify the calculation for theoretical *Hp,* we made the following assumptions: 1) that there are *N* possible reads mapping to any given window; 2) they are evenly distributed across all SNPs; 3) they are assigned to alleles at the haplotype frequency (*F*); 4) the SNPs all differentiate haplotypes in the window perfectly. The formula for computing the theoretical *Hp* from the frequency was derived as such:

$$Hp = \frac{2\sum n_{MAJ}\sum n_{MIN}}{\left(\sum n_{MAJ} + \sum n_{MIN}\right)^2} \qquad [\mathbf{1}](\text{Original formula})$$

$$\sum n_{MAJ} \cong F(N);\ \sum n_{MIN} \cong (1-F)N;\ \ N \cong \sum n_{MAJ} + \sum n_{MIN} \quad [\mathbf{2}](\text{Substitutions})$$

$$Theoretical\ Hp\ = \frac{2(F)(N)(1-F)(N)}{N^2} = 2(F)(1-F) \qquad [\mathbf{3}](\text{Final Thoretical } Hp)$$

For the most conservative scenario (Note Table 1; simulation scenario 2), in which the highest haplotype frequency after 50 generations of breeding was 0.846 (Supplementary Figure 4A; Note Table 1), the theoretical lowest *Hp* would be 0.1549. An analysis of *Hp* values in our experimental data showed that there are 514 out of 9151 (5.62%) windows that would reach this *Hp* value in the tame population. At our cut-off for *Hp* of 0.06611 in the tame population (Supplementary Table 6), only 96 out of 9151 (1.05%) windows were reported as significant. Although the real *Hp* values are expected to be lower than the theoretical values, at our chosen cut-off for *Hp* (0.06611) we identify only ~20% of windows in the most conservative simulation scenario that would be called significant if we used the theoretical value as a cut off.

These results indicate the *Hp* cut-off that we used in our analysis would identify genomic regions with higher haplotype fixation than would be expected through genetic drift in the population without the influence of selection, even in the most conservative simulation scenario.

We also computed the theoretical frequencies for the cut-off values of *Hp* that we used in the experiment by applying formula 3. All of the theoretical haplotype frequencies obtained from the experimental cut-offs (Note Table 2) are higher than the value of 0.846 that we observed in the most conservative simulation scenario (Note Table 1; scenario 2). Additionally, the theoretical haplotype frequencies obtained from the experimental cut-offs are much higher than the base simulation maximum of 0.521 (Note Table 1; scenario 1). We purposely chose a very stringent cut-off to report the strongest candidate regions in this study.

Note Table 2: Theoretical haplotype frequency associated with the experimental Hp cut-off used for each population.

Population	Cut-off Used	Associated Theoretical Haplotype Frequency
Tame	0.06611	0.966
Aggressive	0.10033	0.947
Conventional	0.14815	0.919

Estimation of haplotype lengths in simulated populations.

The lengths of the haplotypes that were Identical-by-Descent with the founder haplotypes were calculated for every haplotype in every individual in the final generation. The haplotype lengths were recorded for all 100 replicates of each simulation scenario. The proportion of the genome represented by haplotypes of a given size or shorter was calculated and is shown in Supplementary Figure 5. The distribution of the average haplotype lengths along chromosome 1 was calculated by dividing the chromosome into one hundred 2.2 Mb windows and averaging the lengths of all haplotypes that have a midpoint falling in the window (Supplementary Figure 6). Fox chromosomes show strong pericentromeric suppression, resulting in a distribution of haplotype lengths that was uneven along the chromosome (Supplementary Figure 6).

Comparison of the simulation scenarios in which the population size and the number of starting haplotypes differed from the base model showed that these parameters had a negligible effect on the length of the haplotypes in the final generation (generation 50). The number of

generations, in contrast, did have an effect, with more generations leading to shorter haplotypes (Supplementary Figure 5). In all simulated scenarios in which the population was bred for 50 generations, the proportion of the genome represented in haplotypes of 500 kb or less was about 1.3%. In simulation scenarios where the population was bred for 100, 250, and 500 generations, the proportion of the genome represented in haplotypes of 500 kb or less was 4%, 12%, and 21%, respectively (Supplementary Figure 5). Overall, these results indicate that a selective sweep scan of fox populations that were bred for 50 generations with a window size of 500 kb would underestimate the level of homozygosity only for a very small part of the genome, justifying the choice of window size used in this study.

***Summary*:** Simulation scenarios 1-6 (Note Table 1) are most closely related to the real demography of the tame and aggressive fox populations. Although we cannot reliably estimate the level of relatedness of the founders of each population, it is unlikely that these populations were started with less than 50 founding haplotypes (Note Table 1; simulation scenario 5). Breeding records provided us with a good estimation of the number of breeders and the number of generations. Although the lowest number of generations we modeled was 50, it is on the high end of plausible values because, due to overlapping generations, the actual number of generations in both tame and aggressive popualtions by 2010 was lower than the number of years separating 2010 from the beginning of the experiment. No haplotypes reached fixation across all simulations with 50 generations of breeding. These simulations also showed that the *Hp* cut-off used in our study is stringent and that the size of the window is appropriate.

Supplementary Note 2. Gene-dropping simulations.

In order to estimate the significance of the cut-off in the F_{ST} analysis of the tame and aggressive populations ($F_{ST}TA$), gene-dropping simulations (MacCluer et al., 1986; Jung et al., 2006) were performed following Wang et al., under review. Pedigree and breeding information for the tame and aggressive populations has been kept since the beginning of the breeding program. Using this information, the 10 tame re-sequenced individuals were traced back to 33 female and 30 male founders of the tame population, and the 10 aggressive re-sequenced individuals were traced back to 38 female and 46 male founders of the aggressive population.

To perform the gene dropping simulations, the founders that were identified based on the 10 tame and 10 aggressive individuals were assigned genotypes (described below), and each successive generation was assigned a genotype based on Mendelian segregation of parental alleles. As the F_{ST} analysis in our study was done on windows that likely had little recombination but contained multiple SNPs, the simulations were performed by dropping non-recombining haplotypes through the pedigree to model the windows in the paper. Therefore, the original assignment of genotypes to the founders for each of the 10,000 simulations was done by generating 50 haplotypes of 1,500 SNPs each (the average number of SNPs in each window in the experimental dataset was 1,782) and assigning each founder two of those haplotypes at random. For each of the 10,000 simulations, a single set of 50 haplotypes was generated and used for both the tame and aggressive strains. We chose to assign haplotypes in this manner to allow for the possibility that the founding animals were related, within and between the strains, and some of them would have the same haplotype.

The minor allele frequency (MAF) of each SNP in the simulated founding haplotypes was assigned independently using the frequency spectrum from the current conventional strain. Although it would be preferred to have direct assessment of the original MAF spectrum, our approach serves as a non-arbitrary starting point to create haplotypes in a more realistic manner.

The F_{ST} of each of the 10,000 simulated windows in the final generation (the 10 tame and 10 aggressive re-sequenced individuals) (Note Figure 1) was calculated using the formula that was used for the experimental re-sequencing data (Karlsson et al., 2007). The mean of the F_{ST} in the simulations was 0.109 (SD 0.046). In comparison, the mean of the $F_{ST}TA$ in the

experimental data was 0.200 (SD 0.111). The highest F_{ST} observed in the simulations was 0.423. The cut-off for significance in the $F_{ST}TA$ analysis of the experimental data was 0.458. None of the 10,000 simulations reached the cut-off for significance in the experimental data, indicating that our choice of a cut-off was stringent.

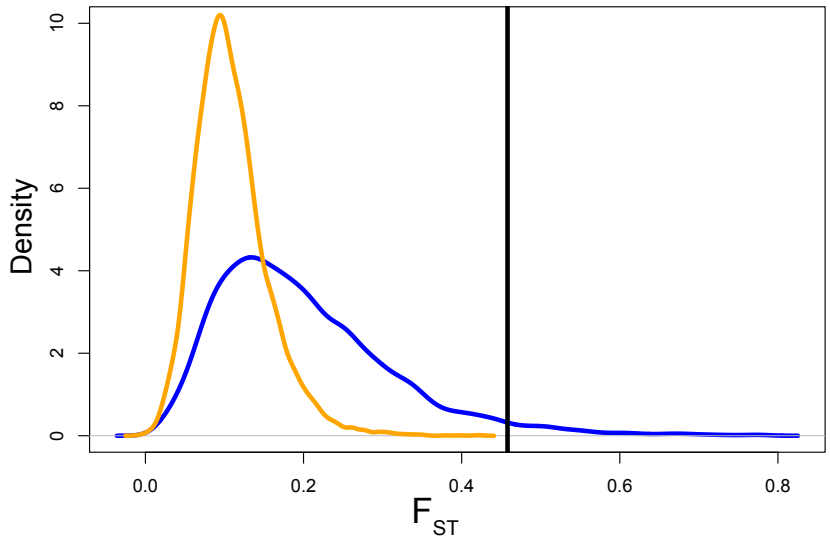

Note Figure 1. Density plots of the F_{ST} values for tame and aggressive populations in simulations (orange) and experimental data (blue). The heavy black vertical line is the cut-off for significance used in the analysis of experimental data (0.458).

Supplementary Note 3. Fine mapping of the region on VVU15 containing *SorCS1* gene.

Using re-sequencing data, we identified 25 short insertions/deletions distributed relatively equally across a 5 Mb interval on scaffold 1, which is syntenic to CFA28: 16,797,450-21,839,153 bp (Supplementary Table 19). Identified polymorphisms were genotyped with fluorescent primers in F2 pedigrees and additional samples from tame (n=64) and aggressive (n=70) foxes.

The analysis of genotypes in the tame population using Haploview grouped eight markers located within and in close proximity to the *SorCS1* gene (scaffold1:41,647,754-42,312,608 bp, CFA28:18,389,720-19,052,218 bp) into one linkage disequilibrium (LD) block (Supplementary Figure 9). Within this LD block Haploview identified one haplotype (*olv*) with frequency 60.6% in the tame population that was not observed in the aggressive population (Table 1; Supplementary Table 20). Two other haplotypes (*trq* and *lav*) formed by these markers were most often observed in the aggressive population and the fourth common haplotype (*pch*) was seen in both populations (Table 1; Figure 4). Additionally there were four more, uncommon haplotypes which do not reach 10% frequency in either population. All eight haplotypes were observed in the F2 pedigrees but only for three main haplotypes (*olv*, *trq*, and *lav*) we observed at least 10 homozygous individuals (Table 1). In the F2 population, the differences in behavior of F2 individuals homozygous for any of the three main haplotypes (*olv*, *trq*, and *lav*) are statistically significant, (Kruskal-Wallis, p=0.03). F2 individuals inherited two copies of the tame haplotype (*olv*) have the highest values for behavior (mean: 0.068) while individuals inherited two copies of the most common aggressive haplotype (*lav*) had the lowest values (mean: -0.546) (Table 1; Figure 4; Supplementary Figure 10). A post-hoc Dunn's test with Benjamini-Hochberg correction achieved a p=0.0142 for the comparison of *lav* and *olv* homozygotes (Figure 4), while other pair-wise comparisons of homozygotes for main haplotypes were not significant (p>0.2).

Haplotype analysis of five markers (scaffold1: 40,049,127-40,603,587 bp, CFA28: 16,797,450-17,348,410 bp) located on the left end of the mapped interval and containing the *SorCS3* gene identified 13 haplotypes in tame and aggressive populations. Three haplotypes (*re*, *gr*, *yl*) were common (reached at least 10% frequency in either population) and were present in the homozygous state in F2 pedigrees (Table 1; Supplementary Table 20). No

significant differences in behavior of F2 individuals homozygous for any of the three haplotypes were observed (Kruskal-Wallis, p=0.44) (Supplementary Figure 10). Haplotype analysis of six markers on the right side of the interval (scaffold1:44,453,503-45,131,383 bp, CFA28:21,165,254-21,839,153 bp) overlapping with five genes (*XPNPEP1*, *ADD3, MXI1, SMNDC1*, and *DUSP5*) identified 10 haplotypes in tame and aggressive populations. Five haplotypes (*r*, *p*, *h*, *s*, *b*) were common (frequency of >10% in either population) but only two had enough homozygous F2 individuals to analyze (*p*, *s*) (Table 1; Supplementary Table 20). The differences in behavior of F2 individuals homozygous for these two haplotypes were also not significant (Kruskal-Wallis, p=0.18) (Supplementary Figure 10).

Supplementary Figure 1. Karyotype of male fox Reef whose genome was sequenced. **(A).** GTG-stained chromosomes of Reef. The chromosomes are numbered according to the nomenclature of Makinen (1985). Framed are the Y-chromosome and supernumerary chromosomes (B-chromosomes) from other Reef's cells bearing 1, 2 and 3 B- chromosomes. **(B).** CBG-stained chromosomes of Reef. **(C, D).** Localization of telomeric repeats (red signals) and nucleolar organizer regions (green signals) in the genome of Reef. Black diamonds indicate centromere positions. Note that telomeric repeats are identified at the ends of all chromosomes and in the centromeric regions of all chromosomes except VVU7, VVU11, VVU13, and VVUX. Red arrows point out the localization of interstitial telomeric repeats in VVU3p and VVU13q.

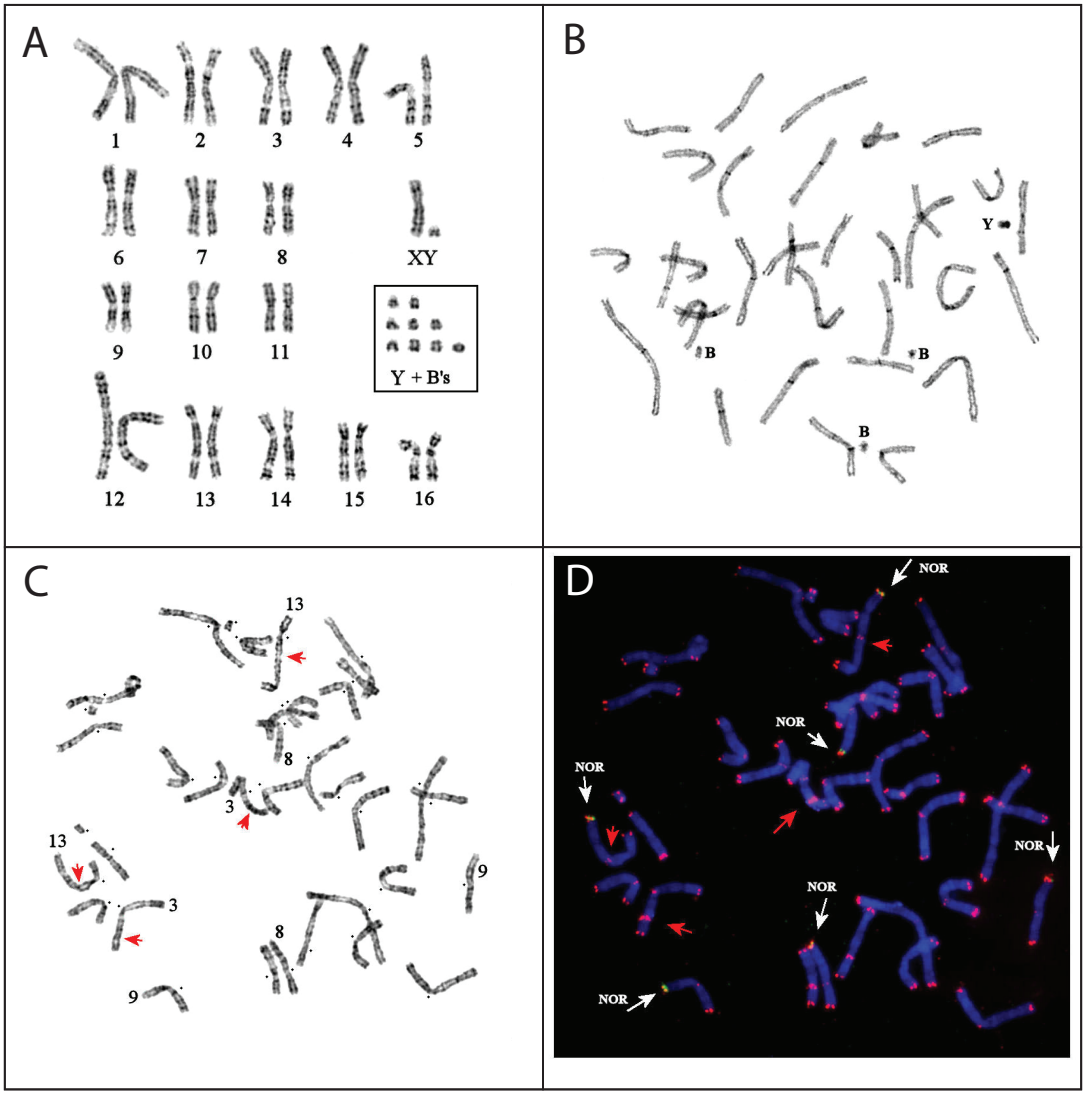

Supplementary Figure 2. Alignment of fox scaffolds against CanFam3.1 with LAST. Examples of scaffolds aligned against one (A) or two dog chromosomes (B).

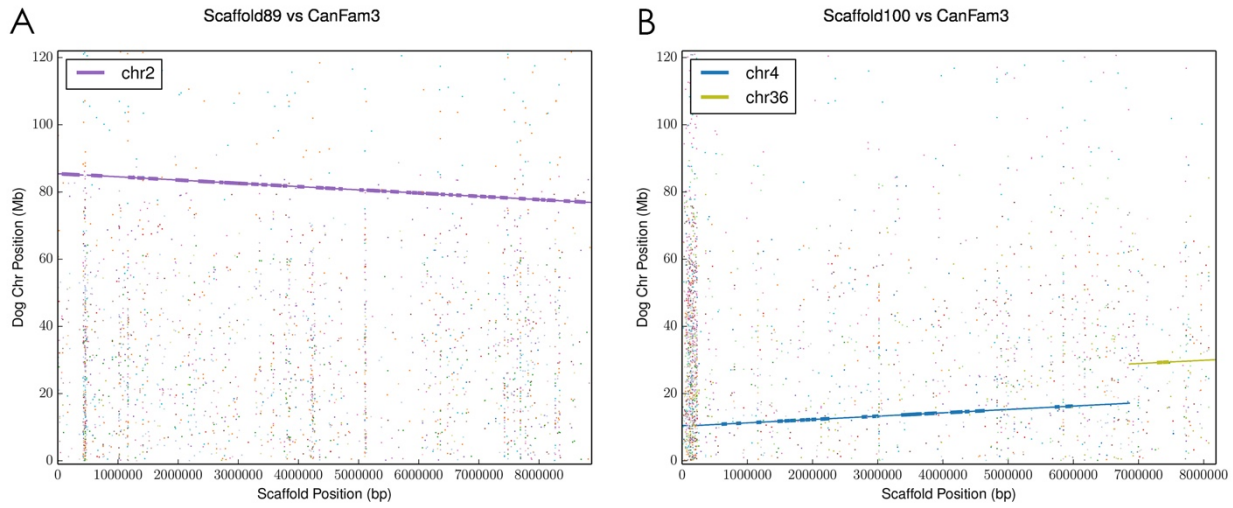

Supplementary Figure 3. The pattern of recombination along fox chromosome 1 (VVU1). The chromosomal length (*x*-axis) and recombination map (*y*-axis) were approximated using the meiotic linkage map of VVU1 aligned against the dog genome. The map from Kukekova et al., 2012 is shown in orange, as an experimental map, and the smoothed map used in the simulations is shown in red.

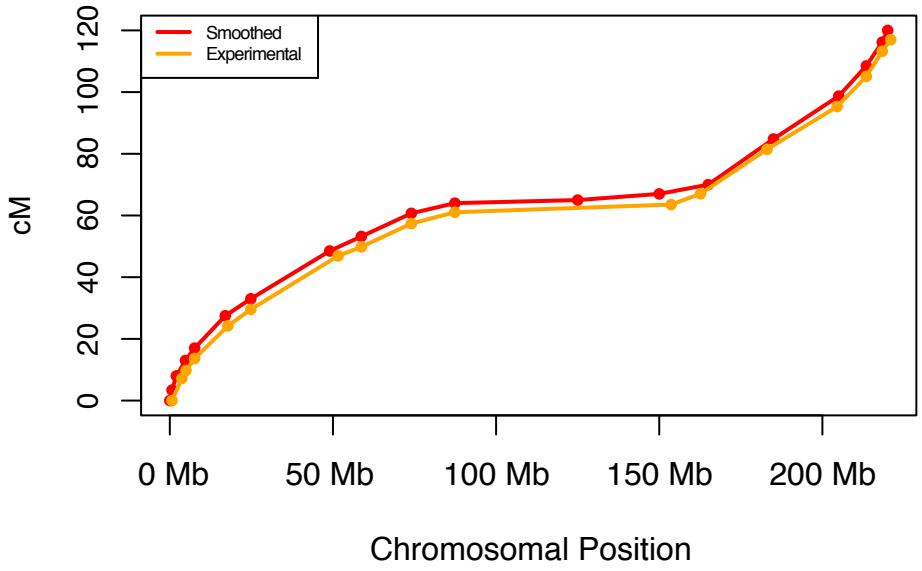

Supplementary Figure 4. The distribution of haplotype frequencies in nine simulation scenarios described in Supplementary Note 1. For each simulated scenario the distribution of haplotype frequencies observed in the final generation across the 100 replicates are presented.

A-C, Graphs: the *x*-axis shows haplotype frequencies; the *y*-axis shows the density of the haplotype frequencies. The colored dot on the baseline is the maximum frequency achieved for that particular simulation scenario. In all graphs, the base simulation is in grey.

D-F, Violin Plots: the violin plots show the same distributions as the graphs; the *y*-axis shows the haplotype frequencies, the *x*-axis shows the haplotype density; the base simulation is in grey.

A/D. Simulations across different population sizes. The breeding population was half (120 individuals; yellow line), twice (480; orange) and four times (960; brown) of the estimated breeding population size (240 individuals; grey). Each population was bred for 50 generations.

B/E. Simulations across different numbers of haplotypes in the founding population. The number of haplotypes was reduced to represent 100 founding haplotypes (dark green) and 50 founding haplotypes (light green) distributed evenly among the 240 founding individuals, in comparison to the base simulation (grey) that included 240 founding individuals with 480 unique haplotypes. Each founding population was bred for 50 generations.

C/F. Simulations across different numbers of generations. The number of generations was two times (100 generations; blue), five times (250 generations; lilac), and ten times (500 generations; purple) the estimated number of generations (50 generations; grey). Each population included 240 unrelated individuals.

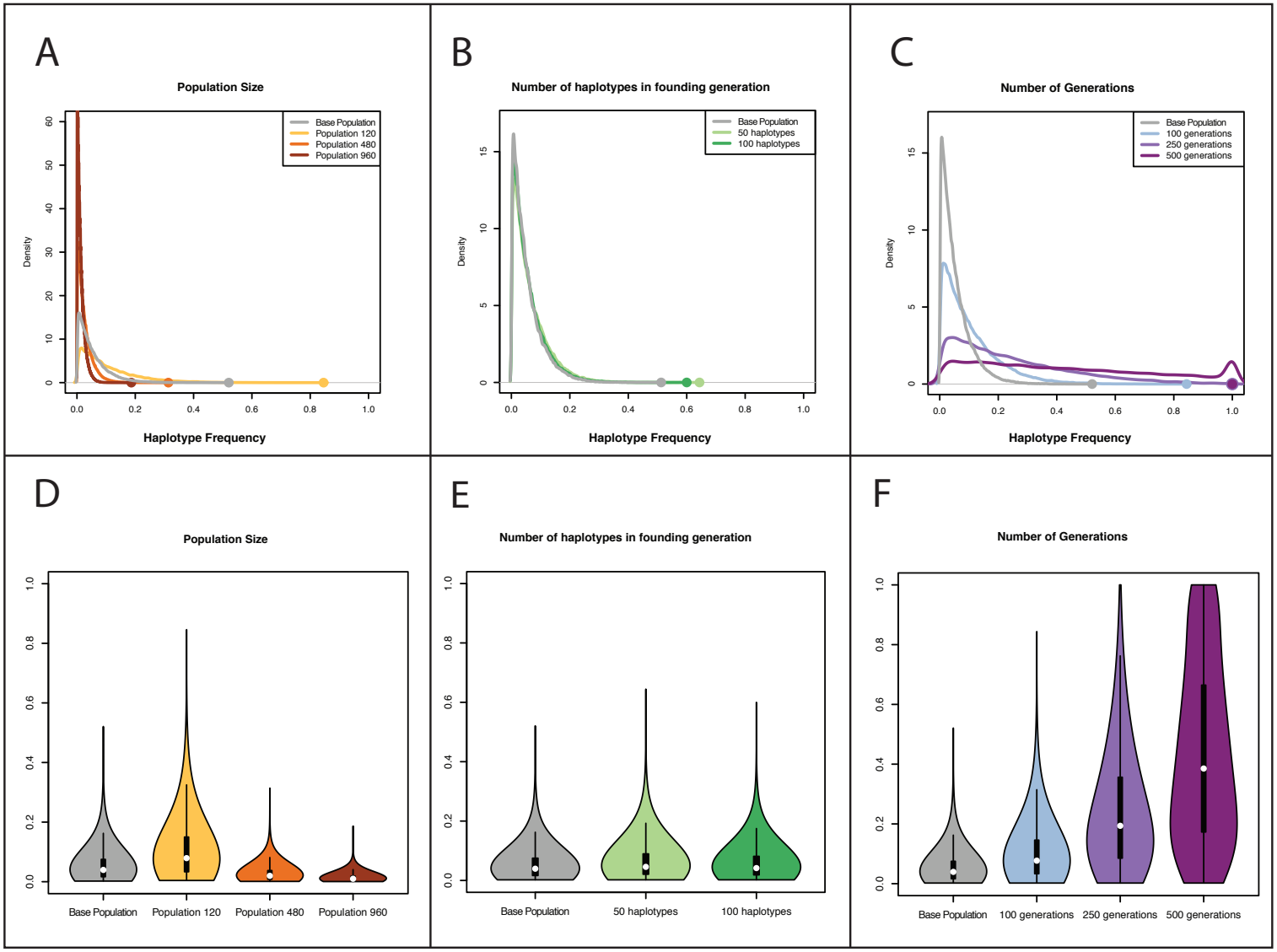
A
Population Size
Base Population
Population 120
Population 480
Population 960
Density
Haplotype Frequency
B
Number of haplotypes in founding generation
Base Population
50 haplotypes
100 haplotypes
Density
Haplotype Frequency
C
Number of Generations
Base Population
100 generations
250 generations
500 generations
Density
Haplotype Frequency
D
Population Size
Base Population
Population 120
Population 480
Population 960
E
Number of haplotypes in founding generation
Base Population
50 haplotypes
100 haplotypes
F
Number of Generations
Base Population
100 generations
250 generations
500 generations

Supplementary Figure 5. Estimation of haplotype length in nine simulation scenarios described in Supplementary Note 1. The *x*-axis is the length of the haplotypes on a log scale, the *y*-axis is the proportion of the genome that is covered by the haplotypes of a given length or smaller. The vertical black line indicates 500 kb, the window size that was chosen for the analysis of pooled heterozygosity (*Hp*). The graph shows the proportion of the genome in each simulation scenario that would have had haplotypes smaller than the 500-kb window size and thus in which the level of homozygosity would have been underestimated. The colors match those used in Supplementary Figure 4.

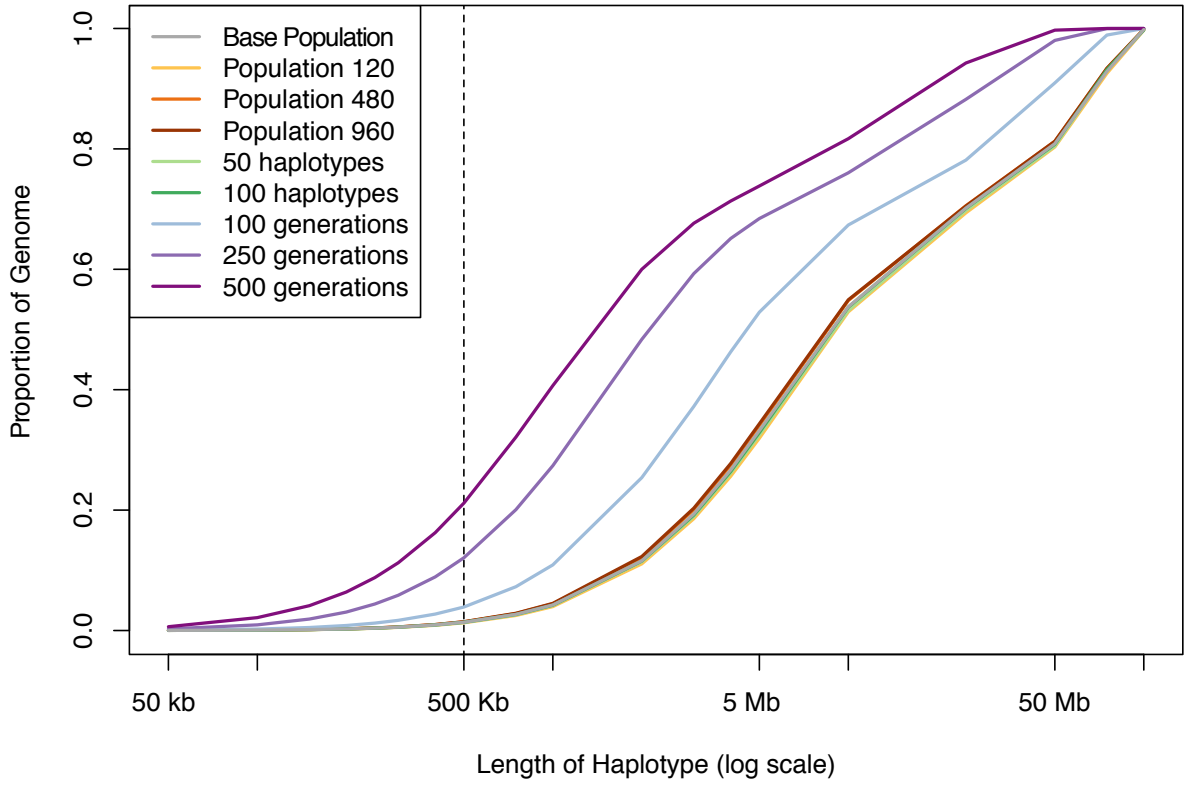

Supplementary Figure 6. Distribution of haplotype lengths along fox chromosome 1. The average length of the haplotypes is plotted along the length of the chromosome. All haplotypes from all individuals across all 100 replicates of each scenario (Supplementary Note 1) are included. The chromosome is divided into one hundred 2.2-Mb windows, and all haplotypes that have a midpoint that falls in the window are included and their lengths averaged. The *x*-axis is the position on the chromosome and the *y*-axis is the average length of the haplotypes that have a midpoint at that position. The horizontal black line is at 500 kb, which was the size of the windows used in this study. As is seen for metacentric fox chromosomes, the middle of the chromosome exhibits a reduced rate of recombination. This is reflected in the lengths of the haplotypes in the pericentromeric region.

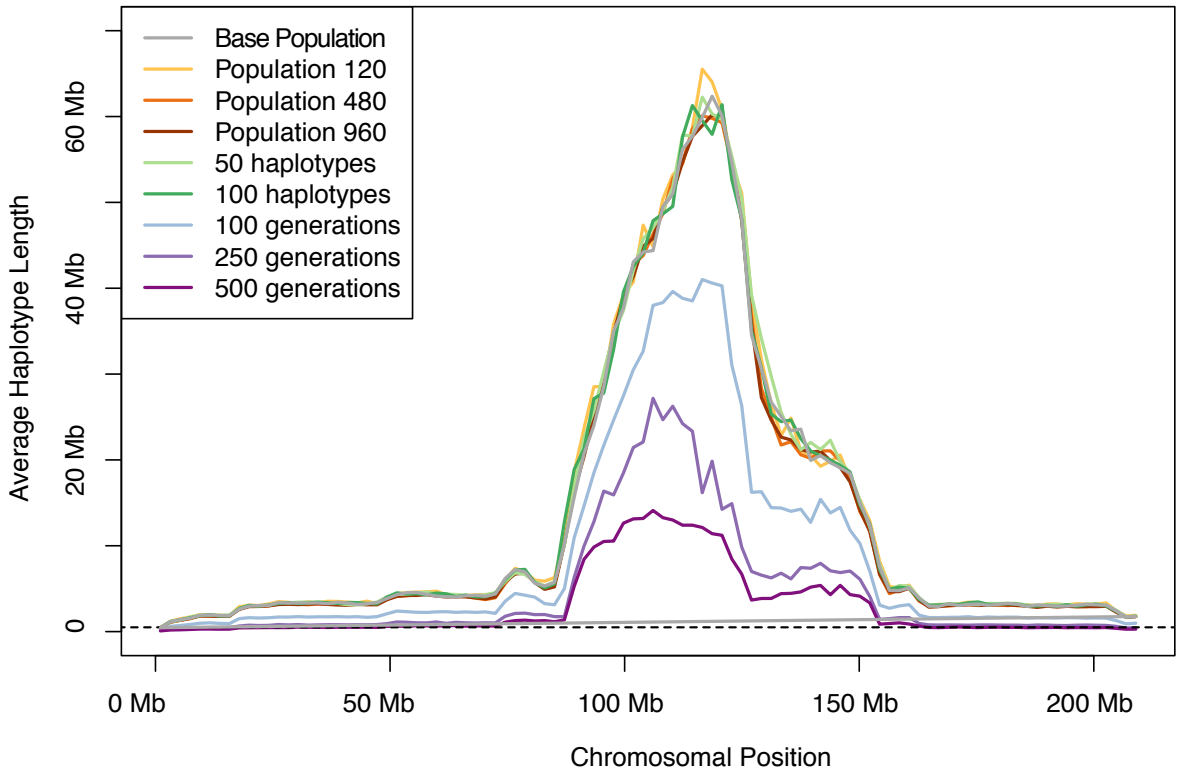

Supplementary Figure 7. Size distributions of combined windows identified in *Hp* and F_{ST} analyses of fox populations. Significant windows identified in the same analysis *(HpT, HpA, HpC,* $F_{ST}TA$, $F_{ST}TC$, or $F_{ST}AC$) were merged into combined windows when the windows were located on the same scaffold and the gap between the windows was not larger than 1 Mb. After merging procedure all significant windows were called combined windows (even if the window was not merged with other windows) to highlight the overall number of genomic regions identified in each analysis *(HpT, HpA, HpC,* $F_{ST}TA$, $F_{ST}TC$, or $F_{ST}AC$).

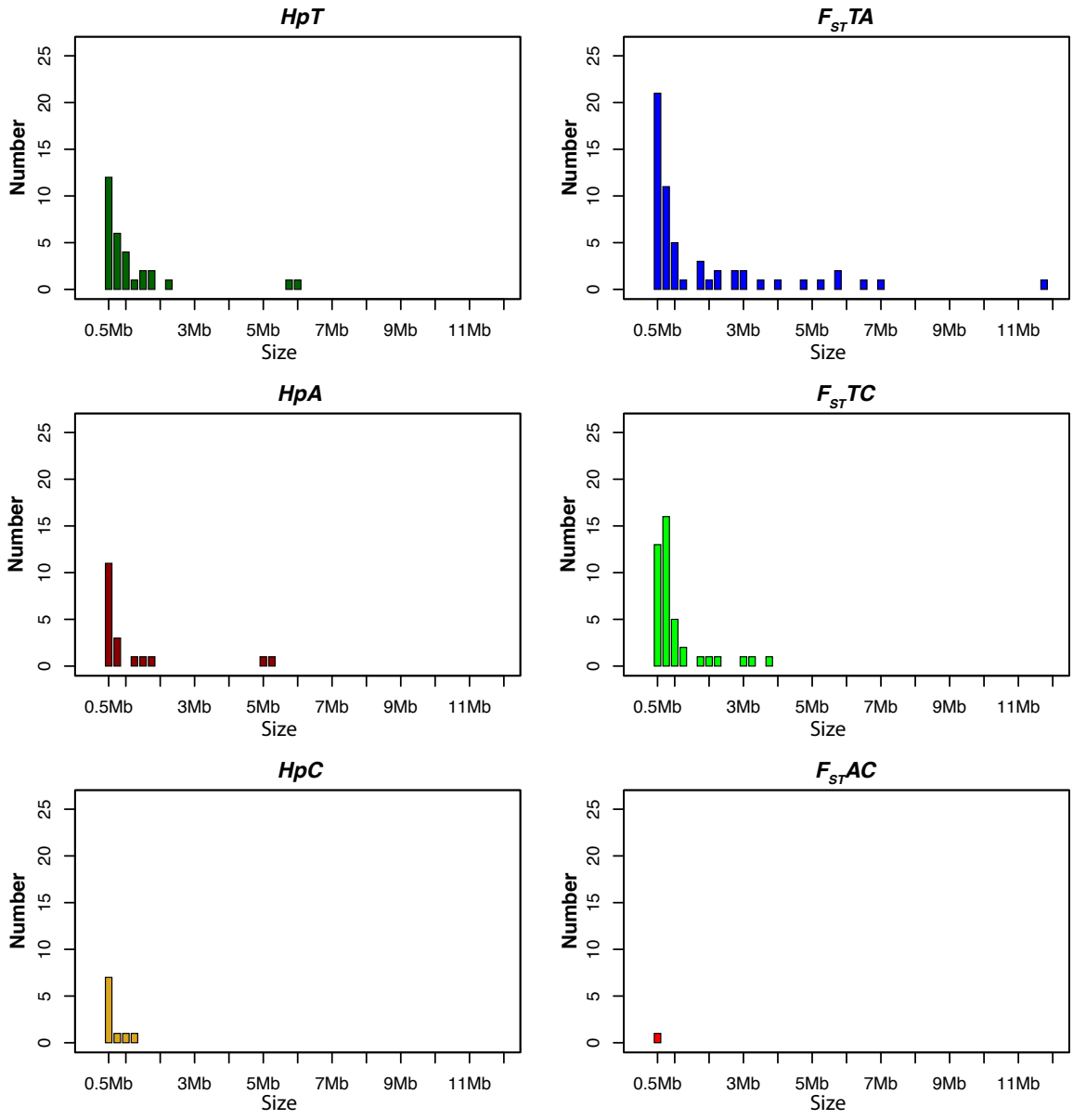

Supplementary Figure 8. Distribution of *CACNA1C* SNP alleles in tame, aggressive, and conventional populations. The frequency is estimated using read count per allele per population. Reference alleles are marked by orange color and fox specific alleles are marked by blue color on both sides of the figure.

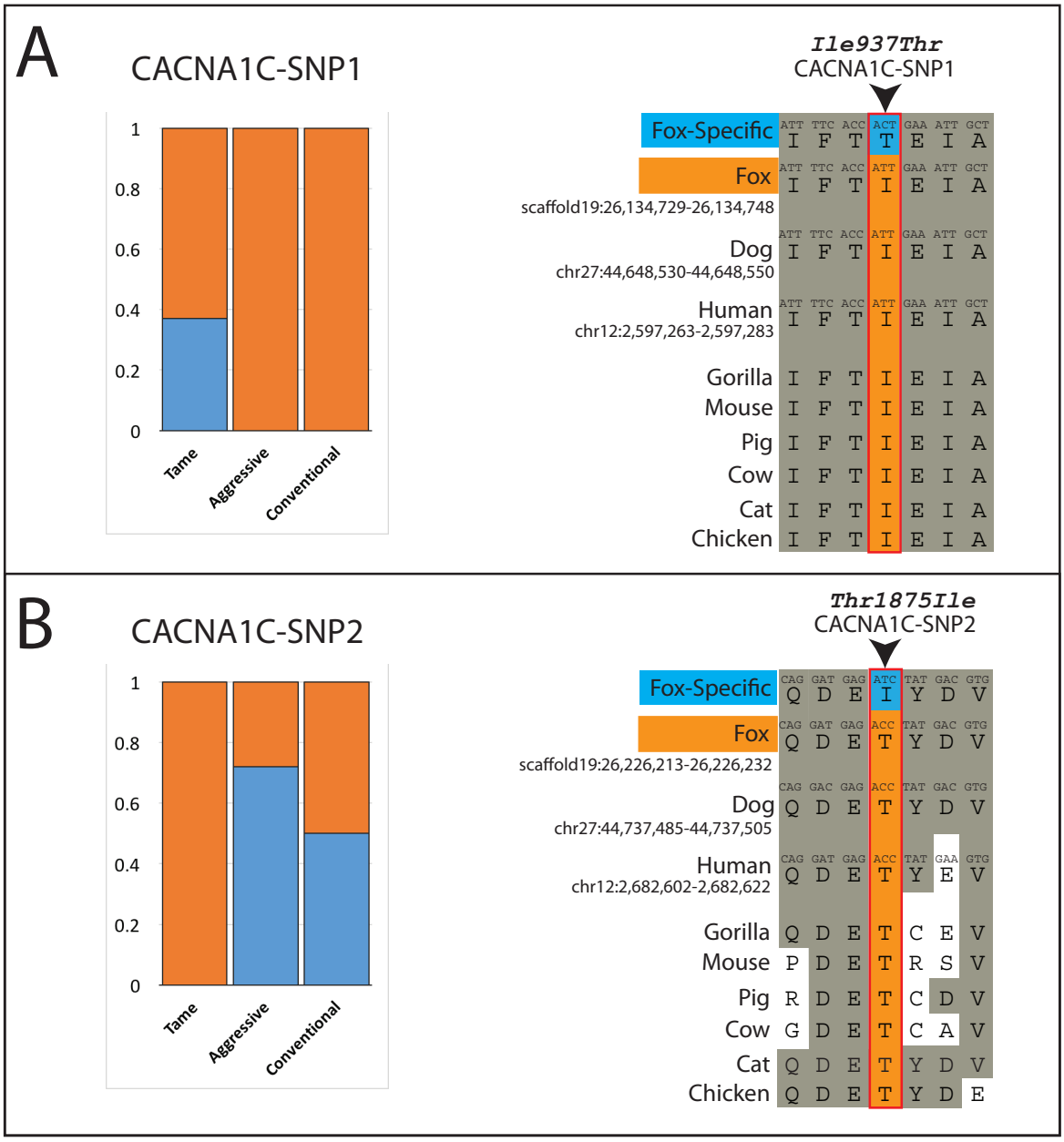

Supplementary Figure 9. Haploview analysis of genotypes along VVU15 in the tame and aggressive populations. The relative order of the genotyped markers on fox scaffold 1 is shown. This region in the fox genome is syntenic to dog chromosome 28 (CFA28). The region with the strongest LD in tame population identified by Haploview is indicated.

Tame

scaffold1:40,049,127- 45,131,383 ; CFA28:16,797,450- 21,839,153

SorCS3 *SorCS1* *XPNPEP1* *MXI1* *DUSP5* *ADD3* *SMNDC1*

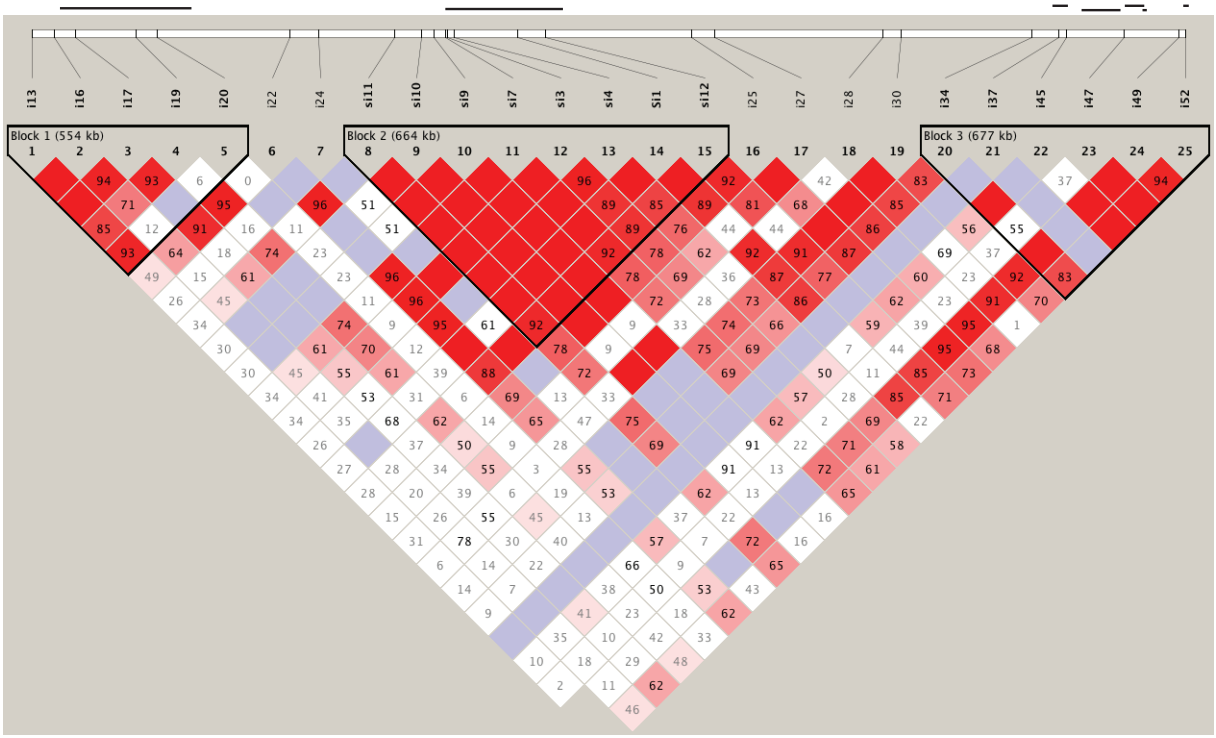

Aggressive

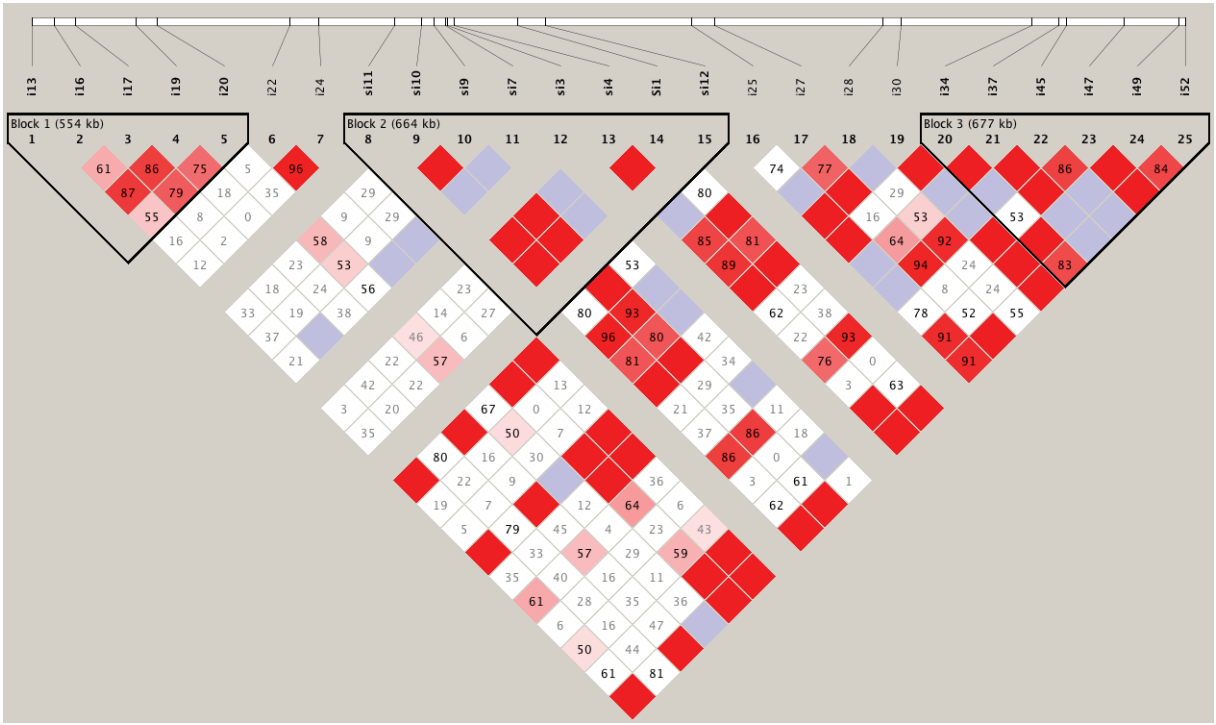

Supplementary Figure 10. Cumulative distributions of D.PC1 values among F2 individuals homozygous for the main haplotypes (Table 1). Only haplotypes with more than 10 F2 homozygous individuals are shown. Each point on the graph represents a single F2 fox. The *y*-axis is the D.PC1 score. The *x*-axis is a rank of individuals in each population. Individuals are evenly spaced on the *x*-axis and ranked, from lowest to highest, by their respective D.PC1 scores. The grey dotted line is the cumulative distribution of the D.PC1 scores of all the F2 foxes. Please see Supplementary Note 3 for details.

A. The cumulative distributions of D.PC1 scores for F2 individuals homozygous for the Left haplotypes. This region overlaps the *SorCS3* gene. **B. The cumulative distributions of D.PC1 scores for F2 individuals homozygous for the Middle (*SorCS1*) haplotypes.** This region overlaps the *SorCS1* gene. Note the large difference between the haplotypes *olv* and *lav*, especially at the midpoint. **C. The cumulative distributions of D.PC1 scores for F2 individuals homozygous for the Right haplotypes.** This region includes the *XPNPEP1*, *ADD3, MXI1, SMNDC1* and *DUSP5* genes. While there is a difference in the lower part of the distribution, the two groups are very similar in the higher points of the distribution.

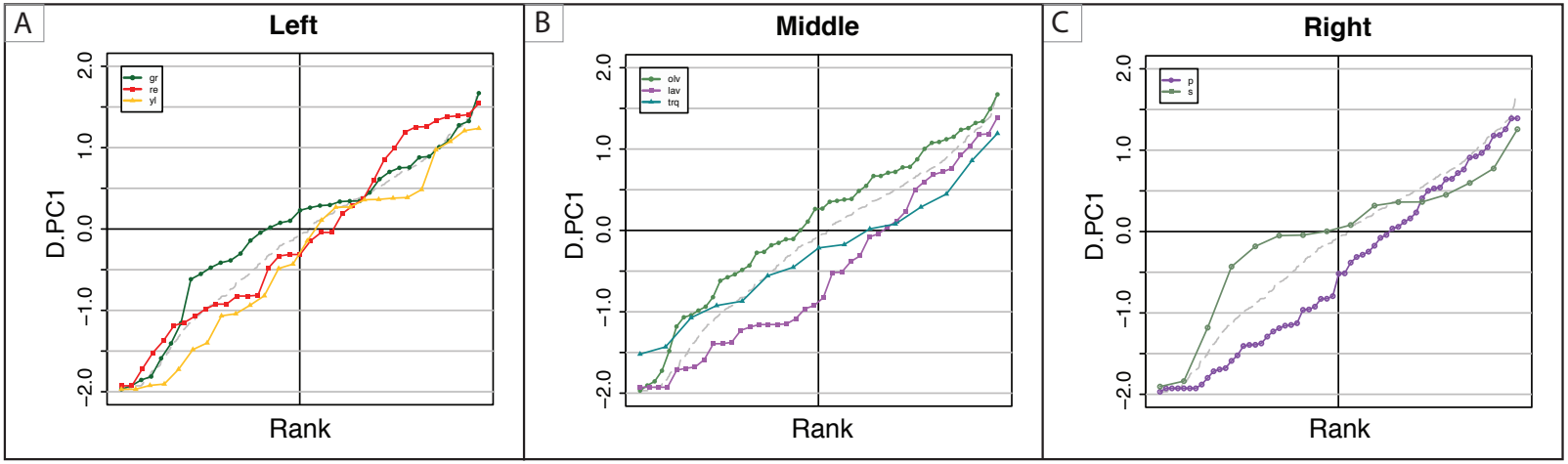
A
Left
B
Middle
C
Right
D.PC1
Rank
2.0
1.0
0.0
−1.0
−2.0
gr
re
yl
olv
lav
trq
p
s

Supplementary Figure 11. Distribution of pooled heterozygosity (*Hp*) values and minimum values from 10,000 permutations. The horizontal axis is the *Hp* value, the vertical axis is the density. The tame population is indicated by the green line, the aggressive population by the red line, and the conventional population by the gold line. The *Hp* distributions obtained for each of the three populations are in darker colors than the distributions built using permuted values. The vertical dotted lines indicate the cutoff value used in the manuscript (green, tame = 0.06611; red, aggressive = 0.10033; gold, conventional = 0.14815).

(A) Distribution of *Hp* values in each of the three populations. The *Hp* values for the 9,151 windows analyzed in each of the populations are presented. The *Hp* distribution in all three populations is non-normal, with all three having a tail to the left. The skew is more pronounced in the tame population. All three populations have their highest point at a very similar value for *Hp*, with the tame population having the lowest value of the three.

(B) Permutation of *Hp* values in each of the three populations. The allele frequencies were permuted 10,000 times, and the value for *Hp* was calculated in every window with >= 20 SNPs. The minimum value observed in each permutation was recorded. The distribution of these minimum values is shown. In contrast to the distributions of the real data, the peaks differ noticeably between the distributions of permuted minimum *Hp* across the populations. The 0.0001 percentile of the minimum *Hp* of the permutations, as calculated by R, was used as the cutoff value for the real data and is indicated by vertical dashed lines (green, tame = 0.06611; red, aggressive = 0.10033; gold, conventional = 0.14815). Note: The *x*-axis is the same for all graphs, and the *y*-axis scale for graphs B-E is comparable although the scale for the *y*-axis of graph A is different.

(C-E). Distribution of original *Hp* values and permuted *Hp* values in each of the three populations. The three populations are graphed separately, with the real data and the minimum *Hp* of the permutations superimposed.

Permutations are a method for using the available data to estimate the likely range of values that would be observed under a neutral model (where no regions differed from any others). The cutoff value chosen, the 0.0001 percentile of the minimum of permutations, means that we would expect, if the distribution of the allele frequencies occurred by chance, less than

one significant window in our set of 9,151 windows. We found 96 Tame, 60 Aggressive, and 14 Conventional windows with *Hp* values below the cutoff. We cannot be certain if the differences in the populations are due to drift or selection. The locations of the peaks of the distributions of the three populations in the real data is very similar. This pattern is consistent with the breeding strategy that was carried out during the development of the strains, where foxes were kept as outbred as possible while placing the tame and aggressive populations under strong selection. The small shift to the left in the tame vs the conventional population is likely indicative of drift or inbreeding. There is a large difference in the left tail of the distribution. This skew could be caused by selection or by drift acting unevenly over the genome. This fat tail is what drives the shift in the distributions for the tame population and lowers our tame cutoff value. The cutoff value was chosen to be very conservative and to allow for robust conclusions even if a large proportion of the tail is caused by drift. Even though the tame population has the lowest cutoff value, it has the highest number of significant windows. It is also the population that has been under intense selection for the longest time.

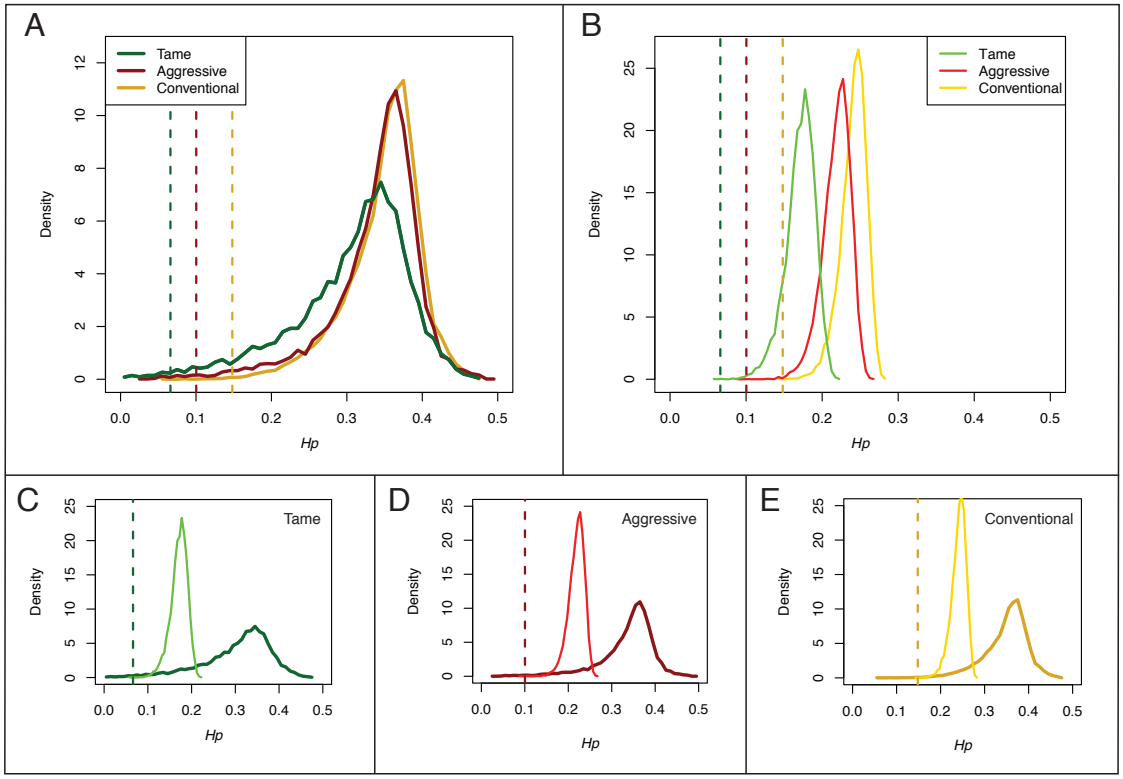

Supplementary Table 1. Fox sequencing and assembly statistics.

A. The amount of sequencing produced for libraries with different insert sizes.

Pair-end libraries	Insert size	Reads length	Raw data		High quality data**	
			Total data (Gb)	Sequence depth* (X)	Total data (Gb)	Sequence depth* (X)
Illumina reads	170bp	100	71.87	29.95	61.04	25.43
	250bp	150	44.72	18.63	38.33	15.97
	500bp	100	43.33	18.05	36.51	15.21
	800bp	150	48.76	20.32	31.68	13.20
	2kb	49	47.52	19.80	26.71	11.13
	5kb	49	38.12	15.88	13.15	5.48
	6kb	49	18.05	7.52	5.43	2.26
	10kb	49	37.18	15.49	10.89	4.54
	20kb	49	17.32	7.22	1.65	0.69
Total	-	-	366.87	152.86	225.39	93.91

* assuming the Genome Size is 2.4 Gb

** after filtering the raw data

B. Fox genome assembly statistics.

Total length of the assembly	2,495,544,672 bp
Contig N50	20,012 bp
Scaffold N50	11,799,617 bp
Longest scaffold	55,683,013 bp
Average scaffold size	3,686 bp
Total number of scaffolds	676,878

Supplementary Table 2. Fox genome annotation statistics.

A. Statistics of predicted protein-coding genes.

	Number	Average transcript length (bp)	Average CDS length (bp)	Average length of introns per gene (bp)	Average length of exons per gene (bp)	Average number of exons per gene
Genes	21,418	29,510	1,479	3,813	177	8

B. Gene function annotation statistics.

	Number	Percent (%)
Total	21,418	
InterPro	18,345	85.65
KEGG	16,308	76.14
Swissprot	20,668	96.50
TrEMBL	21,019	98.14
Annotated	21,028	98.18
Unanotated	390	1.82

Supplementary Table 3. Dog chromosomes syntenic to the fox scaffolds. Cases where a scaffold may overlap a historical fusion event, thereby corresponding to two dog chromosomes but a single fox chromosome, are highlighted. The ID numbers of corresponding scaffolds are in bold.

Separate Excel file.

Supplementary Table 4. The amount of sequencing data produced and mapped to the fox assembly for 30 re-sequenced foxes from the three populations.

Separate Excel file.

Supplementary Table 5. Fox SNPs identified with ANGSD and GATK. The number of SNPs identified by GATK and ANGSD after quality filtering.

Method	ANGSD	GATK	SNPs identified by both methods
Number of SNPs	14,022,690	8,861,724	8,458,133

Supplementary Table 6. Pooled heterozygosity (*Hp*) analysis. A) The *Hp* value cut-offs that would be appropriate for each population, for varying p-values, as established by permutation. Permutation was performed separately for each of the three populations (Supplementary Figure 11). **B)** The number of low *Hp* windows identified in each of three populations at each cut-off. The highlighted column represents the threshold *Hp* value at the p-value cut-off used in each of the three populations (A), and the number of significant *Hp* windows identified in these populations (B). Given that the total number of analyzed windows is 9,151, the p-value for α = 1/10,000 was selected as an appropriate cut-off due to the low number of expected false positives associated with this alpha (1 per population).

A. *Hp* value cut-off for various p-values								
P-value	**0**	**0.00001**	**0.0001**	**0.001**	**0.01**	**0.05**	**0.25**	**0.5**
Tame	0.05600	0.05701	0.06611	0.09209	0.11442	0.13495	0.16016	0.17338
Aggressive	0.08955	0.09062	0.10033	0.14404	0.16575	0.18523	0.20802	0.22108
Conventional	0.14128	0.14197	0.14815	0.17019	0.19232	0.21005	0.23129	0.24332
B. Number of windows that reach each threshold								
Tame	74	76	96	176	267	387	555	682
Aggressive	44	47	60	136	205	294	415	499
Conventional	11	11	14	31	77	130	252	345

Supplementary Table 7. **Significant windows, combined windows, and regions.**

All significant *Hp* and F_{ST} windows are listed. The first column indicates the region, which is the largest unit of conglomeration. 103 regions of the fox genome were identified in which any class of significant windows (*Hp* or F_{ST}) were located on the same scaffold at a distance of 1 Mb or less. Regions are separated by thick lines. The second column is the fox chromosome on which the window is most likely to be located. The fox chromosomal assignments are based on the LASTZ mapping of the fox windows to the dog genome and on known dog/fox synteny. Different fox chromosomes are highlighted in different colors. Fox chromosomes are numbered VVU#.#. The first number, before the period, is the fox chromosome, the second number, after the period, is the chromosomal segment based on the dog/fox synteny, i.e.: fox chromosome 3 is a fusion of dog chromosomes 36, 34, and 6, and VVU03.1 is the segment of VVU3 that corresponds to CFA36, VVU03.2 is the segment that corresponds to CFA34, and VVU03.3 is the segment that corresponds to CFA6. The next six columns indicate the statistic(s) that are significant in the window. These columns also identify combined windows, with gray boxes combining two cells in a column or more. Combined windows were formed when windows significant for the same statistic were identified on the same fox scaffold with gaps not more than 1 Mb. Empty cells highlighted in gray indicate that the corresponding window is not significant for that statistic itself but falls within a combined window. Columns representing these statistics are as follows: *HpT* = significant *Hp* window in the tame population, *HpA* = significant *Hp* window in the aggressive population, *HpC* = significant *Hp* window in the conventional population; $F_{ST}TA$ = significant window identified in the F_{ST} analysis of tame and aggressive populations, $F_{ST}TC$ = significant window identified in the F_{ST} analysis of tame and conventional populations, and $F_{ST}AC$ = significant window identified in the F_{ST} analysis of aggressive and conventional populations. The next three columns to the right provide information about the scaffold number and the start and end of the window on that scaffold. Then, six columns provide *Hp* and F_{ST} values for each window identified in all 103 regions. The colored bars allow the visualization of values obtained for each window. Significant windows are highlighted in gray. The number of SNPs in each window and the average read depth per window are also listed. The corresponding dog chromosome with the start, end, and direction of the window's mapping with LASTZ is also given. Lastly, any genes that were named in the reciprocal best match are listed. Genes that did not receive a name but are in the annotation are listed as Vulp_V######.

Separate Excel File.

Supplementary Table 8. The number of genes identified in significant *Hp* and F_{ST} windows. $F_{ST}TA$: number of genes in windows significant in the F_{ST} analysis of tame and aggressive populations, $F_{ST}TC$: tame and conventional populations, $F_{ST}AC$: aggressive and conventional populations; *HpT* - number of genes in windows identified as significant in the *Hp* analysis of tame population, *HpA* – aggressive population, *HpC* - conventional population. The intersections indicate the number of genes overlapping between two analyses. A number of genes with gene symbols are listed without parenthesis; the total number of genes (a number of genes with and without gene symbols) are listed in parenthesis.

	$F_{ST}TA$	***$F_{ST}TC$***	***$F_{ST}AC$***	***HpT***	***HpA***	***HpC***
$F_{ST}TA$	650 (894)	136 (177)	0	32 (46)	74 (95)	5 (8)
$F_{ST}TC$		234 (303)	0	10 (18)	39 (50)	9 (12)
$F_{ST}AC$			3 (3)	0	0	3 (3)
HpT				138 (185)	0	0
HpA					159 (205)	5 (8)
HpC						51 (63)

Supplementary Table 9. PANTHER overrepresentation statistics. Only overrepresentation test results with $p<0.05$ after Bonferroni correction are reported. Three genes which were common to all GO terms identified in the analyses of *HpT* windows are underlined. Related terms are highlighted with same color. PANTHER Version 13.0 released on 2017-11-12.

Separate Excel File.

Supplementary Table 10. Identification of brain expressed genes both from significant windows and a complete list of annotated genes in 9,151 windows. The Human Protein Atlas, Version 17 (http://www.proteinatlas.org) was used to identify brain-expressed genes both from significant windows and a complete list of annotated fox genes. Brain tissues were considered to be caudate, cerebellum, cerebral cortex, hippocampus, hypothalamus, and pituitary gland. No overrepresentation for brain-expressed genes in significant windows was observed (p-value =0.69 based on a hypergeometric test).

Gene set	**Total**	**In the Human Protein Atlas**	**In the Human Protein Atlas and brain-expressed**	**Percent of brain-expressed genes**
Genes in the Human Protein Atlas	12,976	12,976	10,424	80.3%
Annotated Genes in 9,151 fox windows	15,826	10,991	9,058	82.4%
Annotated Genes in fox significant windows (*Hp* and F_{ST})	971	698	571	81.8%

Supplementary Table 11. Genes from significant windows identified in KEGG database for glutamatergic, serotonergic, dopaminergic, GABAergic, and cholinergic synapses.

Genes from significant windows	KEGG-04724; Glutamatergic synapse	KEGG-04726; Serotonergic synapse	KEGG-04728; Dopaminergic synapse	KEGG-04727; GABAergic synapse	KEGG-04725; Cholinergic synapse
CACNA1C	Glutamatergic	Serotonergic	Dopaminergic	GABAergic	Cholinergic
CAMK4					Cholinergic
CHRM3					Cholinergic
CHRNA7					Cholinergic
GABARAPL1				GABAnergic	
GABBR1				GABAnergic	
GABRA3				GABAnergic	
GABRQ				GABAnergic	
GAD1				GABAnergic	
GNB3	Glutamatergic	Serotonergic	Dopaminergic	GABAnergic	Cholinergic
GNG4	Glutamatergic	Serotonergic	Dopaminergic	GABAnergic	Cholinergic
GRIN2B	Glutamatergic		Dopaminergic		
GRM6	Glutamatergic				
KCNJ3	Glutamatergic	Serotonergic	Dopaminergic		Cholinergic
MAPK9			Dopaminergic		
NRAS		Serotonergic			Cholinergic
PIK3R2					Cholinergic
PLCB1	Glutamatergic	Serotonergic	Dopaminergic		Cholinergic
PLCB4	Glutamatergic	Serotonergic	Dopaminergic		Cholinergic
TRPC1	Glutamatergic	Serotonergic			

Supplementary Table 12. Genomic regions identified in the analysis of pooled heterozygosity (*Hp*) and fixation index (F_{ST}). The windows with significant *Hp* values are combined into combined *Hp* windows when there is no gap larger than 1 Mb between significant windows and the windows belong on the same scaffold. Same rule was applied for merging significant F_{ST} windows into combined F_{ST} windows. The number of regions and scaffolds and the chromosomes containing significant windows are listed. See Supplementary Table 7 for details.

Type of window	Number of combined windows	Number of regions	Number of scaffolds	Fox chromosomes	Length of the longest region in the fox genome
HpT	30	29	21	3, 4, 6, 7, 8, 11, 12, 13, 14, 16	6.00 Mb
HpA	19	18	15	1, 3, 4, 7, 8, 12, 14	5.13 Mb
HpC	10	10	9	1, 3, 4, 10, 12, 14	1.25 Mb
$F_{ST}TA$	57	56	48	1, 2, 3, 4, 6, 7, 8, 9, 10, 11, 12, 13, 14, 15, 16, X	11.75 Mb
$F_{ST}TC$	42	38	30	1, 3, 4, 6, 7, 8, 10, 11, 12, 14, X	3.75 Mb
$F_{ST}AC$	1	1	1	14	0.50 Mb

Supplementary Table 13. Comparison of 103 regions of interest identified in the fox with regions under selection in dogs. In three publications, vonHoldt et al., 2010, Axelsson et al., 2013, and Wang et al., 2013, dog regions were listed according to CanFam2. In the table we list the positions of these regions in both CanFam2 and CamFam3.1. Freedman et al., 2016 listed regions in CanFam3.1. Dog regions in green have complete overlap with the fox regions, gold is partial overlap, and red are dog regions that are near the fox regions but not overlapping. Only the fox regions that overlap or are near dog regions are included (45 of 103 regions). Dog regions from Wang et al., 2013 with an asterisk were placed to the best fox match, but they would also fit the criteria for a different fox region and are also listed in a separate column.

Separate Excel File.

Supplementary Table 14. Fox QTL that overlap with 103 genomic regions from Supplementary Table 7. The positions of fox regions from Supplementary Table 7 were compared with positions of nine fox behavioral QTL identified in the previous studies (Kukekova et al., 2011; Nelson et al., 2017). Only QTL for behavioral phenotypes defined using principal component analysis were included in this analysis. A QTL interval was defined as a genomic region extended 5-15 cM in both directions from the QTL peak (cM position of the QTL with the most significant statistical support). The interval boundary on either side of the QTL peak was defined by the position of the mapped microsatellite marker (Nelson et al., 2017) located within the 5-15 cM interval from the QTL peak but being the farthest from the QTL peak. E.g. if there are three markers on the fox meiotic linkage map (Nelson et al., 2017) located on same side from the QTL peak at distances 7, 14, and 17 cM, respectively, the boundary of the QTL interval on this side was placed at the position of the marker located 14 cM from the QTL peak. All microsatellite markers used for QTL mapping are dog-derived markers with known positions in the dog genome. Because current QTL intervals are large and often correspond to several fox scaffolds, we used the locations of the microsatellite markers in the dog genome (Nelson et al., 2017) to define the length and positions of the dog genomic regions syntenic to the fox QTL intervals. These regions were then compared to the dog genomic coordinates of the 103 fox regions from Supplementary Table 7. This analysis identified 30 fox regions which overlap with five out of nine fox behavioral QTL. The percent of the length of the region that shows overlap with a QTL interval is listed.

Separate Excel File.

Supplementary Table 15. Fox orthologs of genes associated with autism spectrum disorders and bipolar disorder in humans and/or found to affect aggression in mouse models that were identified in significant *Hp* and F_{ST} windows. SFARI stands for Simons Foundation Autism Research Initiative.

Genes from four SFARI categories (high confidence, suggestive evidence, strong candidate, syndromic)	**SFARI category**	**Bipolar disorder associated genes from Douglas et al., 2016**	**Genes known to be involved in mouse aggression**
AKAP9	suggestive evidence	*BAZ2B*	*CNGA2*
AMPD1	suggestive evidence	*CACNA1C*	*DCT*
APH1A	suggestive evidence	*CHRNA7*	*KCNJ3*
ATP10A	suggestive evidence	*GNG4*	*NCAM1*
CACNA1C	syndromic	*GPR50*	*PAK7*
CHRNA7	suggestive evidence	*IQGAP2*	*PRNP*
GRIN2B	high confidence	*NCAM1*	
KAT2B	strong candidate	*NTF3*	
MAGEL2	syndromic, strong candidate	*PTPRO*	
MYO9B	suggestive evidence	*RASGRF2*	
PIK3R2	syndromic	*RBFOX1*	
PLCB1	suggestive evidence	*SCAMP1*	
RBFOX1	suggestive evidence	*ZNF385D*	

Supplementary Table 16. Pooled heterozygosity analysis in the region partly syntenic to the Williams-Beuren syndrome region in humans. Significant *HpA* windows are highlighted in gray.

Separate Excel File.

Supplementary Table 17. Missense mutations identified in *CACNA1C, ATP10A, MYO9B, IQGAP2,* and *PTPRO* genes.

Gene	SNP	SNP location in CanFam3.1	SNP type	Dog allele	Amino acid change in dog protein	Number of reads per allele in tame population	Number of reads per allele in aggressive population	Number of reads per allele in conventional population
CACNA1C	**SNP1**	chr27:44,648,540	T/C	T	*Ile*937*Thr*	17T/11C	36T/0C	15T/0C
	SNP2	chr27:44,737,495	C/T	C	*Thr*1875*Ile*	36C/0T	19C/51T	13C/13T
ATP10A	**SNP1**	chr3:35,008,222	A/G	A	*Asp*924*Gly*	9A/20G	32A/36G	36A/3G
	SNP2	chr3:35,027,759	G/A	G	*Val*1416*Met*	7G/27A	20G/36A	29G/3A
	SNP3	chr3:35,027,654	G/A	G	*Ala*1381*Thr*	8A/23G	8A/35G	19A/22G
MYO9B	**SNP1**	chr20:45,525,137	G/T	G	*Gln*1222*Lys*	1G/32T	6G/42T	18G/9T
IQGAP2	**SNP1**	chr3:29,998,116	T/C	T	*Met*330*Val*	9C/17T	22C/6T	0C/34T
PTPRO	**SNP1**	chr27:31,170,591	C/T	C	*Ala*335*Thr*	0C/27T	20C/6T	19C/17T

Supplementary Table 18. Summary of the information obtained for *CACNA1C* and *SorCS1* genes.

Separate Excel File.

Supplementary Table 19. Primer pairs and multiplexes used for genotyping the 5-Mb region on VVU15.

Separate Excel File.

Supplementary Table 20. Haplotypes identified in the 5-Mb interval on VVU15. The frequencies of haplotypes identified in the tame and aggressive populations by Haploview. Only haplotypes with a frequency > 1% in either population are shown. Indel i7 had 4 alleles. Allele 270 was used as allele 1 in the Haploview run, and alleles 272/273/274 were binned as allele 2. After Haploview was run, the individuals with haplotypes that included binned alleles were examined, and the correct allele from the list of binned alleles was chosen. In all cases there was only one allele possible. Haplotypes that are shared between the populations are shaded the same color in both populations.

Separate Excel File.

Supplementary Table 21. Statistics of the STRUCTURE analysis.

A. The detailed statistics. STRUCTURE was run four times for each level of *k*, 1 through 5. The data for each of the four runs at each *k* is shown. At level *k,* the data is separated into *k* clusters. The proportion of the data that was assigned to each cluster is indicated by the right-most columns labeled "inferred clusterN". The order of the clusters is random between runs. The estimated log probability of observing the data given the model was calculated by STRUCTURE. The mean value of the log likelihood is averaged over each of the 100,000 MCMC runs. The variance is the variance of the log likelihood over those runs.

Separate Excel File.

Supplementary Information References:

Abrahams, B.S. *et al.* SFARI Gene 2.0: a community-driven knowledgebase for the autism spectrum disorders (ASDs). *Molecular Autism* **4**, 36 (2013).

Axelsson, E. *et al.* The genomic signature of dog domestication reveals adaptation to a starch-rich diet. *Nature* **495**, 360-4 (2013).

Bhat, S. *et al.* CACNA1C (Cav1.2) in the pathophysiology of psychiatric disease. *Progress in Neurobiology* **99**, 1-14 (2012).

Douglas, L.N., McGuire, A.B., Manzardo, A.M. & Butler, M.G. High-resolution chromosome ideogram representation of recognized genes for bipolar disorder. *Gene* **586**, 136-47 (2016).

Freedman, A.H. *et al.* Demographically-Based Evaluation of Genomic Regions under Selection in Domestic Dogs. *PLoS Genetics* **12**, e1005851 (2016).

Johnson, J.L. *et al.* Genotyping-By-Sequencing (GBS) Detects Genetic Structure and Confirms Behavioral QTL in Tame and Aggressive Foxes (*Vulpes vulpes*). *PLoS One* **10**, e0127013 (2015).

Jung, J., Weeks, D.E., Feingold, E. Gene-dropping vs. empirical variance estimation for allele-sharing linkage statistics. *Genetic Epidemiology* **30**, 652-665 (2006).

Karlsson, E.K. *et al.* Efficient mapping of mendelian traits in dogs through genome-wide association. *Nature Genetics* **39**, 1321-8 (2007).

Kessner, D. & Novembre, J. forqs: forward-in-time simulation of recombination, quantitative traits and selection. *Bioinformatics* **30**, 576-7 (2014).

Kukekova, A.V. *et al.* A meiotic linkage map of the silver fox, aligned and compared to the canine genome. *Genome Research* **17**, 387-99 (2007).

Kukekova, A.V. *et al.* Mapping Loci for fox domestication: deconstruction/reconstruction of a behavioral phenotype. *Behavior Genetics* **41**, 593-606 (2011).

Kukekova, A.V., Temnykh, S.V., Johnson, J.L., Trut, L.N. & Acland, G.M. Genetics of behavior in the silver fox. *Mammalian Genome* **23**, 164-77 (2012).

MacCluer, J.W., Vandeberg, J.L., Read, B., Ryder, O.A. Pedigree Analysis by Computer-Simulation. *Zoo Biology* **5**, 147-160 (1986).

Makinen, A. The standard karyotype of the silver for (Vulpes fulvus Desm.). Committee for the standard karyotype of Vulpes fulvus Desm. *Hereditas* **103**, 171-6 (1985).

Nelson, R.M. *et al.* Genetics of Interactive Behavior in Silver Foxes (Vulpes vulpes). *Behavior Genetics* **47**, 88-101 (2017).

Rubin, C.J. *et al.* Whole-genome resequencing reveals loci under selection during chicken domestication. *Nature* **464**, 587-91 (2010).

Sanders, S.J. *et al. De novo* mutations revealed by whole-exome sequencing are strongly associated with autism. *Nature* **485**, 237-41 (2012).

vonHoldt, B.M. *et al.* Genome-wide SNP and haplotype analyses reveal a rich history underlying dog domestication. *Nature* **464**, 898-902 (2010).

Wang, G.D. *et al.* The genomics of selection in dogs and the parallel evolution between dogs and humans. *Nature Communications* **4**, 1860 (2013).

Wang, X. *et al*. Genomic responses to selection for tame/aggressive behaviors in the silver fox (*Vulpes vulpes*). bioRxiv 228544; doi: https://doi.org/10.1101/228544 (2018).